Numerical Analysis of Index-Guiding Photonic Crystal Fibers with Low Confinement Loss and Ultra-Flattened Dispersion by FDFD Method

M. Pourmahyabadi* and Sh. Mohammad Nejad*

Abstract: In this article, perfectly matched layer (PML) for the boundary treatment and an efficient compact two dimensional finite-difference frequency-domain (2-D FDFD) method were combined to model photonic crystal fibers (PCF). For photonic crystal fibers, if we assume that the propagation constant along the propagation direction is fixed, three-dimensional hybrid guided modes can be calculated by using only a two-dimensional mesh. An index-guiding PCF with an array of air-holes surrounding the silica core region has special characteristics compared with conventional single-mode fibers (SMFs). Using this model, the fundamental characteristics of single mode photonic crystal fibers (SMPCFs) such as confinement loss, bending loss, effective mode area and chromatic dispersion are numerically investigated. The results revealed that low confinement loss and zero-flattened chromatic dispersion can be obtained by varying the air-holes diameter of each ring along the PCF radius. In this work, an especial PCF with nearly zero-flattened dispersion (1.3 ps/nm/km) over a wide wavelength range which covers O, E, S, C, L and U telecommunication wavelength bands and low confinement loss (0.06 dB/km at 1.55μm) is designed. Macro-bending loss performance of the designed PCF is also studied and it is found that the fiber shows low bending losses for the smallest feasible bending radius of 5 mm. Also, it is revealed that the temperature sensitivity of PCFs is very low in compared with the conventional fibers.

Keywords: Bending loss, Finite difference frequency domain, Dispersion, Large mode area, Photonic crystal fiber.

1 Introduction

Photonic crystals have attracted a great deal of attention in the optics community in recent years. One of the most promising applications of photonic crystals is the possibility of creating compact integrated optical devices with photons as the carriers of information, and then the speed and bandwidth of advanced communication systems can be increased dramatically [1-2].

Photonic crystal fibers (PCFs), a kind of two dimension photonic crystals, consisting of a central defect region surrounded by multiple air-holes that run along the fiber length are attracting much attention in recent years because of unique properties which are not realized in conventional optical fibers. PCFs are divided into two different kinds of fibers. The first one is index-guiding PCF, guiding light by total internal reflection between a solid core and a cladding region with multiple air-holes. The second one uses a perfectly periodic structure exhibiting a photonic band-gap (PBG) effect at the operating wavelength to guide light in a low index core-region. Index-guiding PCFs, also called holey fibers or microstructure optical fibers, possess especially attractive property of great controllability in chromatic dispersion [3-5]. All of these properties are related to the fiber design, namely, the pitch (Λ) of the periodic array, the air-holes diameter (d) and the number of air-holes rings around the core (N) [6-9].

Here, we proposed PCFs that simultaneously exhibit low confinement losses and ultra-flattened dispersion over a wide wavelength range which covers O, E, S, C, L and U telecommunication wavelength bands.

This paper is organized as follows: In the next section, the theory of FDFD is described. Section 3

Iranian Journal of Electrical & Electronic Engineering, 2009.
Paper first received 21 Jan. 2009 and in revised form 5 Apr. 2009.
* The Authors are with the Nanoptronics Research Lab, Department of Electrical Engineering, Iran University of Science and Technology, Tehran , Iran.
E-mails: Pmahyabadi@iust.ac.ir, Shahramm@iust.ac.ir.

focuses on the fundamental properties of PCFs such as guided modes, confinement loss, chromatic dispersion and effective mode area. In section 4, fiber geometry structures and then the numerical results are discussed. Finally the paper sets out its conclusion in the last section, section6.

2 Analysis Method

The finite difference frequency domain (FDFD) is popular and appealing for numerical electromagnetic simulation due to its many merits. It has been one of the major tools for the analysis and understanding of PCFs.

The discretization scheme can be derived from the Helmholtz equations or Maxwell's equations directly. Now we use the direct discretization schemes first described for photonic crystal fibers by Zhu et al [10]. Yee's two-dimensional mesh is illustrated in Fig. 1; note that the transverse fields are tangential to the unit cell boundaries, so the continuity conditions are automatically satisfied. After inserting the equivalent nonsplit-field anisotropic PML in the frequency domain, the curl Maxwell equations are expressed as

$$\begin{aligned} jk_0 s\varepsilon_r E &= \nabla \times H \\ -jk_0 s\mu_r H &= \nabla \times E \end{aligned} \tag{1}$$

$$s = \begin{bmatrix} s_y/s_x & & \\ & s_x/s_y & \\ & & s_x s_y \end{bmatrix} \tag{2}$$

where μ_r and ε_r are the relative permittivity and permeability of the medium considered, $k_0=2\pi/\lambda$ is the wave number in free space, $s_x=1-\sigma_x/j\omega\varepsilon_0$, $s_y=1-\sigma_y/j\omega\varepsilon_0$ and σ is the conductivity profile. Assuming that the PCFs are lossless and uniform and the propagation constant along the z direction is β. Thus, the field variation along the propagation direction z is of the form $exp(-j\beta z)$. The z-derivatives, $\partial/\partial z$, can be replaced by $-j\beta$ in Maxwell's equations and thus three-dimensional equations can be solved using only a two-dimensional mesh. Using the central difference scheme and zero boundary conditions outside of the anisotropic PML layers, the curl equations (1) can be rewritten in a matrix form which includes six field components. Then eliminating the longitudinal magnetic and electric fields, the eigenvalue matrix equation in terms of transverse magnetic fields and transverse electric fields can be obtained as

$$\begin{bmatrix} Q_{xx} & Q_{xy} \\ Q_{yx} & Q_{yy} \end{bmatrix} \begin{bmatrix} H_x \\ H_y \end{bmatrix} = \beta^2 \begin{bmatrix} H_x \\ H_y \end{bmatrix} \tag{3}$$

$$\begin{bmatrix} P_{xx} & P_{xy} \\ P_{yx} & P_{yy} \end{bmatrix} \begin{bmatrix} E_x \\ E_y \end{bmatrix} = \beta^2 \begin{bmatrix} E_x \\ E_y \end{bmatrix} \tag{4}$$

where the Q and P are highly sparse coefficient matrices. The order and the nonzero elements in them are reduced and effectively stored in sparse format, so the computation efficiency is improved greatly. The complex propagation constant β and the transversal magnetic or electric field distribution can be solved out quickly and accurately by a sparse matrix solver [11, 12].

3 Photonic Crystal Fiber Characteristics

3.1 Guided Modes in PCFs

In an index-guiding PCF, the core index is greater than the average index of the cladding because of the presence of air-holes, and the fiber can guide the light by total internal reflection as a standard fiber does. That is, the guided light has an effective index n_{eff} that satisfies the condition

$$n_{co} > n_{eff} = \frac{\beta}{k_0} > n_{FSM} \tag{5}$$

where β is the propagation constant along the fiber axis, n_{co} is the core index, and n_{FSM} is the cladding effective index of the FSM. In the case of a PCF made from pure silica, n_{co} is reduced to the index of silica [13].

In fact, unlike conventional fibers, triangular PCFs can be designed to be Endlessly Single-Mode (ESM), that is to support only the propagation of the fundamental mode whatever the wavelength and the pitch value are. Previous analyses on their cutoff properties have demonstrated that the ESM region is defined by $d/\Lambda<0.406$ [6]. Also if the confinement loss of the higher order modes are much more than that of the fundamental mode and there is a large difference in the effective index between them and the fundamental mode, then these fibers are likely to be single mode in practice [14].

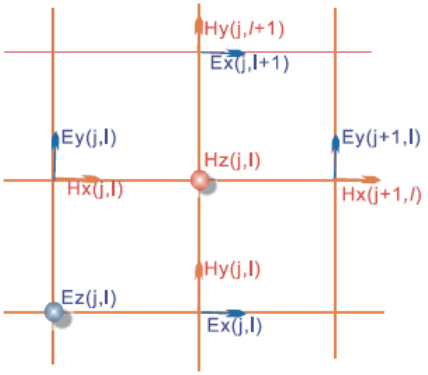

Fig. 1. Unit cell in Yee's 2D-FDFD mesh

3.2 Chromatic Dispersion

PCFs possess the attractive property of great controllability in chromatic dispersion. The chromatic dispersion profile can be easily controlled by varying the air-holes diameter and the air-holes pitch. Controllability of chromatic dispersion in PCFs is a very important problem for practical applications to optical communication systems, dispersion compensation, and nonlinear optics. So far, various PCFs with remarkable dispersion properties have been investigated numerically. The chromatic dispersion D of a PCF is easily calculated from the effective index of the fundamental mode n_{eff} versus the wavelength using

$$D = -\frac{\lambda}{c}\frac{d^2 n_{eff}}{d\lambda^2} \tag{6}$$

where c is the velocity of light in a vacuum. The material dispersion using Sellmeier equation is directly considered in the perturbation formulations [15-17]. When the air-holes diameter to pitch ratio is very small and the air-holes pitch is large, the dispersion curve is close to the material dispersion of pure silica. As the air-holes diameter is increased, the influence of waveguide dispersion becomes stronger [13,18].

3.3 Confinement Loss

The losses in PCFs occur for a number of reasons, such as intrinsic material absorption loss, structural imperfection loss, Rayleigh scattering loss, confinement loss, and so on. Fabrication-related losses can be reduced by carefully optimizing the fabrication process. Confinement loss is an additional form of loss that occurs in single-material fibers [13].

The SiO_2 materials don't have an imaginary component because they materials are not absorbing. PCFs are usually made from pure silica, and so the guided modes are inherently leaky because the core index is the same as the index of the outer cladding without air-holes. Because of the finite transverse extent of the confining structure, the effective index is a complex value; its imaginary part $Im(n_{eff})$ is related to losses L (in decibels per meter) through the relation [19-20];

$$L = \frac{40\pi.\mathrm{Im}\left(n_{eff}\right)\times 10^6}{\lambda.\ln(10)} \tag{7}$$

This confinement loss can be reduced exponentially by increasing the number of air-holes rings that surround the solid core, and is determined by the geometry of the structure. Also, Increasing the air-holes diameter results in the increasing of the air filling fraction which is calculated by the following equation in triangular lattice and consequently decreasing the loss,

$$F = \frac{\pi}{2\sqrt{3}}\left(\frac{d}{\Lambda}\right)^2 \tag{8}$$

It is important to know how many numbers of air-holes rings are required to reduce the confinement loss under the Rayleigh scattering limit for practical fabrication process.

3.4 Bending Loss

The bending losses of PCFs differ qualitatively from those of conventional step index fibers. Like conventional fibers, PCFs exhibit a bend loss edge at long wavelengths due to the fact that the mode extends further into the cladding, resulting in a more weakly guided mode that will suffer a greater perturbation in response to bending. PCFs also possess an additional bend loss edge at short wavelengths as a direct consequence of their novel cladding structure [21-23].

Predictions of macro-bending induced attenuation in photonic crystal fibers have been made using various approaches including antenna-theory for bent standard fibers [24-25], finite difference mode solver with perfectly matched layers [26] and finite difference time-domain (FDTD) techniques [27].

We use a different technique for bend calculation. It is a fully vectorial coordinate transformation technique. The main issue when simulating bends is using PML boundary conditions to absorb the leaked radiation.
Maxwell's equations are solved in a Cartesian coordinate system with the appropriate boundary conditions in FDFD method;

$$\begin{aligned} &\vec{E}(x,y,z) = \vec{f}(x,y)\exp(i\beta z) \\ &\beta = n_{eff}k_0 = n_{eff}\frac{2\pi}{\lambda_0} \end{aligned} \tag{9}$$

In a bent fiber, for achieving modes, cylindrical FDFD is solved using following equation.

$$\begin{aligned} &\vec{E}(\rho,y',\theta) = \vec{f}(\rho,y)\exp(i\beta\rho_0\theta) \\ &\beta = n_{eff}k_0 = n_{eff}\frac{2\pi}{\lambda_0} \end{aligned} \tag{10}$$

where the (ρ,y',θ) represent a cylindrical coordinate system. So for the bend orientation angle of φ, the electromagnetic fields are returned in the Cartesian reference frame $(x,y,z=0)$:

$$\vec{E}(\rho,y',\theta=0) = \vec{E}(x,y,z=0) = \begin{pmatrix} E_x(x,y) \\ E_y(x,y) \\ E_z(x,y) \end{pmatrix} \tag{11}$$

$$\rho - \rho_0 = x.\cos(\varphi) + y.\sin(\varphi)$$
$$y' = -x.\sin(\varphi) + y.\cos(\varphi)$$

The bend leads to radiative losses. The losses can be determined by using Perfectly Matched Layer (PML) boundary conditions to absorb the radiation from the fiber [28-29].

3.5 Effective Mode Area in PCFs

The effective area of the fiber core A_{eff} is defined as,

$$A_{eff} = \frac{\left(\iint_S |E_t|^2 \, dxdy\right)^2}{\iint_S |E_t|^4 \, dxdy} \qquad (12)$$

where E_t is the transverse electric field vector and S denotes the whole fiber cross section [13]. As expected, increasing the air-hole size, the mode becomes more confined, and thus the effective area and the confinement loss are both reduced. Also, increasing the number of air-holes rings, the confinement loss is significantly reduced. On the other hand, the effective area is almost independent of the number of air-holes rings. We can see that the confinement loss contributes significantly to the loss of PCFs when the air-holes pitch Λ is small.

3.6 Temperature Sensitivity

All material properties are specified through the index of refraction. So the influence of temperature variation on the PCF characteristics can be explained by temperature dependency of refractive index. The significance of effects related to thermal expansion and refractive indexes change are governed by the thermal coefficients of both silica $\beta_s = 1.2\times10^{-5}/k^\circ$ and dry air $\beta_h = -0.9\times10^{-6}/k^\circ$ [30-32]. In the following, we also investigate this effect on the PCF behavior. More information is available in [30].

4 Fibers Geometry Structure and Numerical Results

In this section, we will address the modified confinement loss and dispersion curves when the air-holes diameter of each ring along the radius is altered. As shown in Fig. 2(a), all the air-holes in the section of typical PCFs are arrayed according to triangle regularity with identical pitch Λ, spacing of the neighboring air-holes. The scale of the air-holes is denoted by d of its diameter. Because the effective refractive index of the core region is higher than the cladding region, total internal reflective (TIR) can occur in the interface between the core and cladding.

In the following, we will investigate the loss and dispersion characteristics of the designed PCFs. There are three degrees of freedom; air-holes diameter, air-holes pitch; and the number of air-holes rings for controlling the confinement loss and dispersion behaviors.

As above mentioned, finite difference frequency domain method FDFD with a perfect matched layer PML boundary condition is used, applied with Mode Solution software, provided by Lumerical Solutions, Inc [28].

In the operating wavelength λ = 1.55 μm, the transversal field intensity distribution for the fundamental guiding mode of the PCF with Λ=3 μm, d=1.2 μm is shown in Fig. 2(b). The results show the profile of emitted optical power. The intensity of propagated wave is marked by colors; red color/dark shade represent relatively highest intensity of light and blue/bright shade – the lowest one. This PCF is ESM because of $d/\Lambda=0.4<0.406$.

As stated before, the dispersion coefficient D is proportional to the second derivative of the modal effective index with respect to the wavelength λ. For this reason, we have to calculate the dependence of modal effective index n_{eff} with respect to the wavelength λ firstly. Fig. 3 shows the confinement loss and dispersion characteristics as a function of wavelength over a wide wavelength range including O, E, S, C, L and U telecommunication wavelength bands.

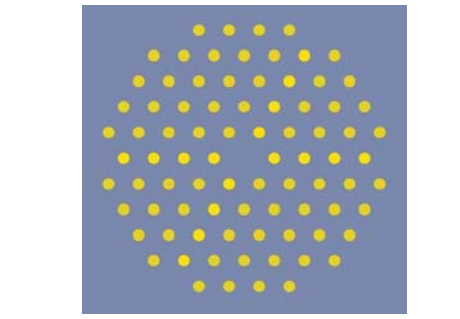

(a)

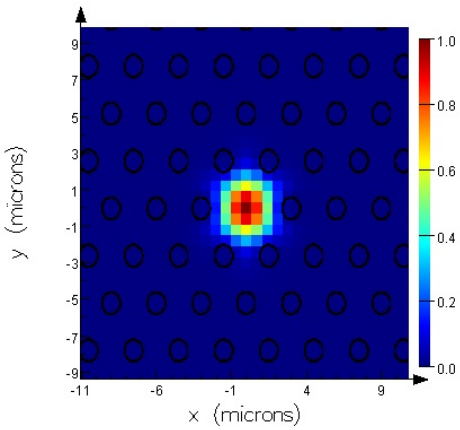

(b)

Fig. 2. (a) Section structure of a typical PCF with Λ=3 μm, d=1.2 μm and N=5 (b) Transversal field intensity distribution for the guiding mode at 1.55 μm wavelength

Consequently, it has relatively high confinement loss, but its dispersion slope is less than 0.012 ps/nm^2/km. It should be mentioned that the dispersion characteristics of PCFs will be improved by eliminating the corner air-holes, whereas the confinement loss will be increased since the index contrast between core and cladding increases. Therefore, in order to decrease the confinement loss, we increase the number of air-holes rings. As it can be seen in Fig. 4, the number of air-holes rings is increased to 7. In this case, the air-hole filling factor and consequently index contrast between the core and the cladding is increased, so the mode is more strongly confined.

The results revealed (Fig. 5) that the confinement loss is reduced to less than 0.001 dB/km, while the chromatic dispersion is slightly increased. In addition to above effects, dispersion slope is reduced to 0.01 ps/nm^2/km. It should be mentioned that the effective mode area is 16.6291 μm^2. Therefore, the confinement loss is reduced exponentially by increasing the number of air-holes rings that surround the solid core.

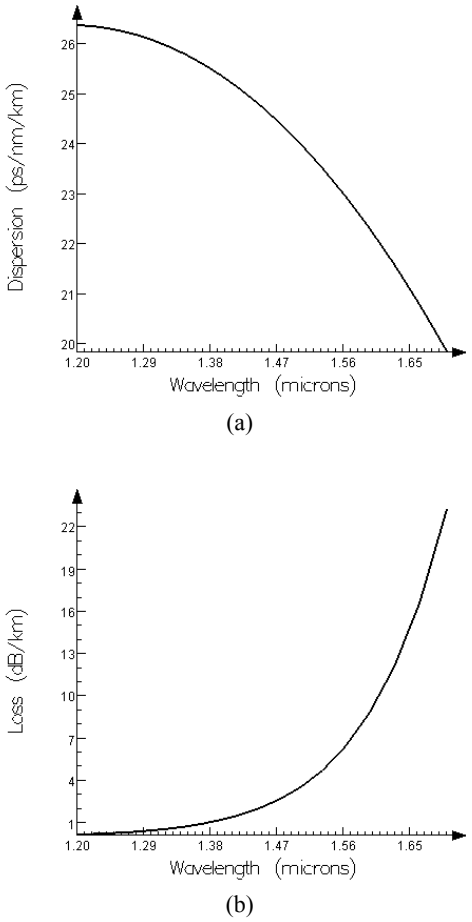

Fig. 3. (a) Confinement loss and (b) Dispersion characteristics as a function of wavelength for the photonic crystal fiber depicted in Fig. 2

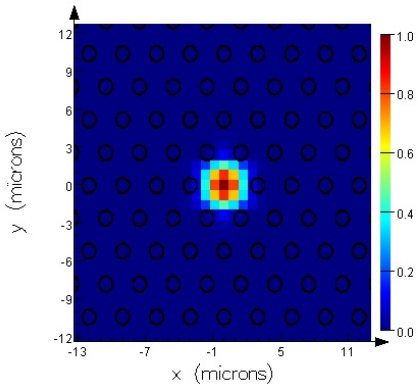

Fig. 4. Transversal field intensity distribution for the guiding mode of a SMPCF with the following parameters; Λ=3 μm, *d*=1.2 μm and *N*=7 at 1.55 μm wavelength

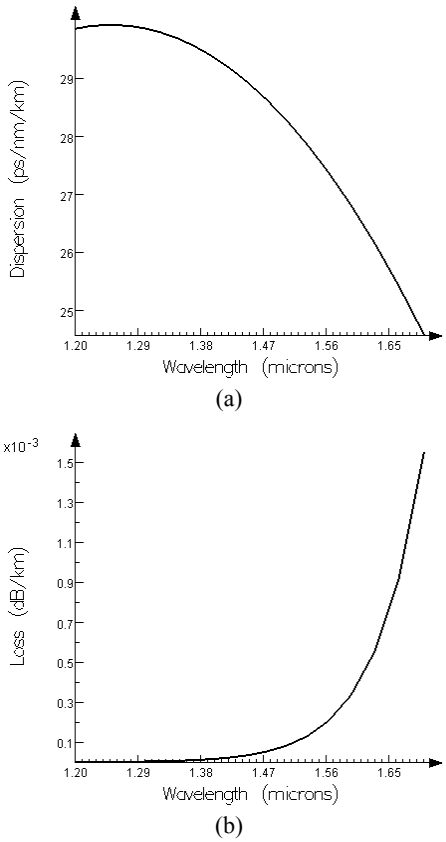

Fig. 5. (a) Confinement loss and (b) Dispersion characteristics as a function of wavelength for the PCF with Λ=3 μm, *d*=1.2 μm and *N*=7

In the next step, in order to modify the dispersion and confinement loss characteristics simultaneously, we change the air-holes diameter of each ring along the radius. Fig. 6(a) shows the cross section of the proposed fiber in which the air-holes diameter of two inner rings is d_1 and the air-holes diameter of the other rings is d_2. The transversal field intensity distribution for the fundamental guiding mode of the PCF with Λ=3 μm,

d_1=2.1 μm and d_2=2.4 μm at 1.55μm wavelength is shown in Fig. 6(b).

Table 1. shows the confinement loss at 1.55 μm wavelength when d_1 is varying from 1.3 μm to 2.7 μm. As it can be seen, the total loss is decreased by increasing the air-holes diameter of two inner rings. Thus, the confinement loss is not only reduced exponentially by increasing the number of air-holes rings that surround the solid core, but also by increasing the air-holes diameter.

By fixing Λ=3 μm, d_2=2.4 μm and changing λ in a wide wavelength range of 1.2 μm~1.7 μm, the characteristics of dispersion are shown in Fig. 7 for different air-holes diameters of two inner rings. As it can be seen, the chromatic dispersion increases when the air-holes diameter of two inner rings increases, and in the best case, it reaches to 28.4 ps/nm/km at the wavelength of 1.55 μm for the PCF with d_1=1.3 μm, but the dispersion slope is the least (0.0034 ps/nm^2/km) for the PCF with d_1=1.7 μm in the wavelength range of 1.2 μm~1.7 μm. It should be mentioned that the variation of d_2 has no remarkable influences on the dispersion characteristics.

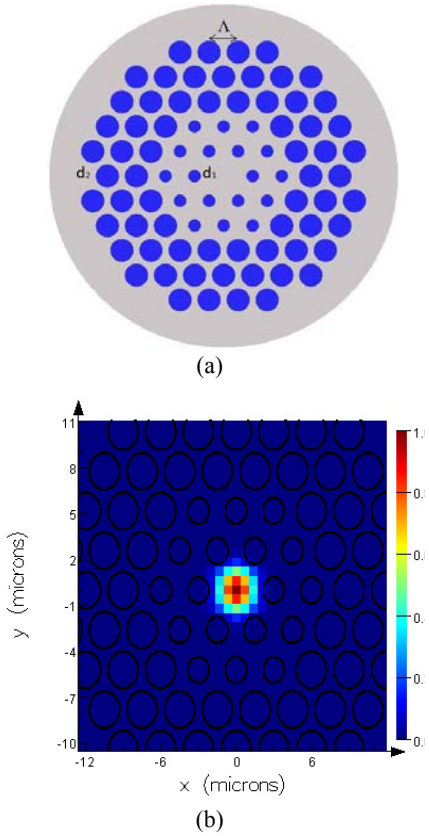

Fig. 6. (a) Section structure of the proposed PCF with Λ=3 μm, d_1=2.1 μm and d_2=2.4 μm (b) Transversal field intensity distribution for the fundamental guiding mode at 1.55 μm wavelength

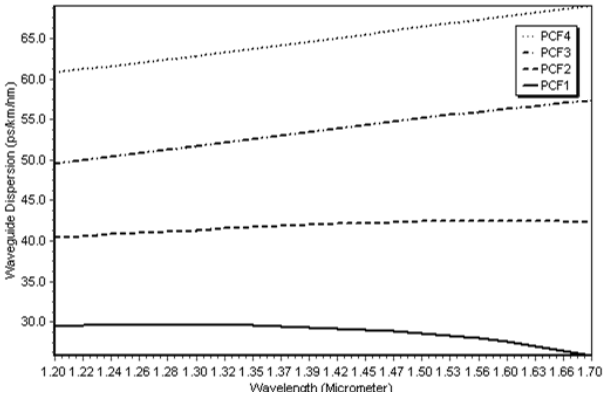

Fig. 7. Dispersion characteristics as a function of wavelength for different photonic crystal fibers with the following parameters; Λ=3 μm, N=5, PCF1: d_1=1.3 μm, PCF2: d_1=1.7 μm, PCF3: d_1=2.1 μm and PCF4: d_1=2.5 μm

Therefore, the air-holes diameter of the inner rings strongly affects on the dispersion and loss characteristics whereas the air-holes diameter of the outer rings just slightly affects on the loss characteristics of PCFs.

Table 1. The confinement loss of PCF as a function of d_1 at 1.55μm wavelength when Λ=3 μm and d_2=2.4 μm

d_1(μm)	Confinement Loss (dB/km)×10^{-7}
1.3	5.8744
1.5	4.8118
1.7	2.3551
1.9	1.7276
2.1	1.0631
2.3	0.7552
2.5	0.6449
2.7	0.5272

Fig. 8 shows the dispersion characteristics at room temperature for a PCF with the following parameters; Λ=3 μm, d_1=1.7 μm and d_2=2.4 μm (solid line). Also the influence of temperature variation of 200 $^{\circ}$K on the dispersion curve is depicted in Fig. 8 (dash line). As it can be seen, dispersion is increased about +1 ps/nm/km because of increasing the refractive index, while the dispersion slope is slightly decreased. In addition, the confinement loss characteristics as a function of wavelength is depicted in Fig. 9. As it is shown in overall the confinement loss is slightly increased by increasing temperature.

In the standard SMF, if the refractive index contrast between core and cladding is more than the critical value, it can't support a single mode anymore. So the refractive index contrast is effected by the high temperature variation and the fiber characteristics may change entirely, but in the PCFs, the characteristics are

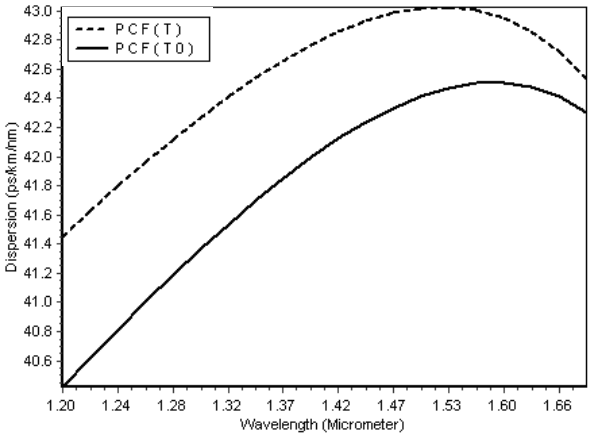

Fig. 8. Dispersion characteristics as a function of wavelength at room temperature (solid line) and at 500ºK (dash line) for PCF with the following parameters; Λ=3 μm, d_1=1.7 μm and d_2=2.4 μm

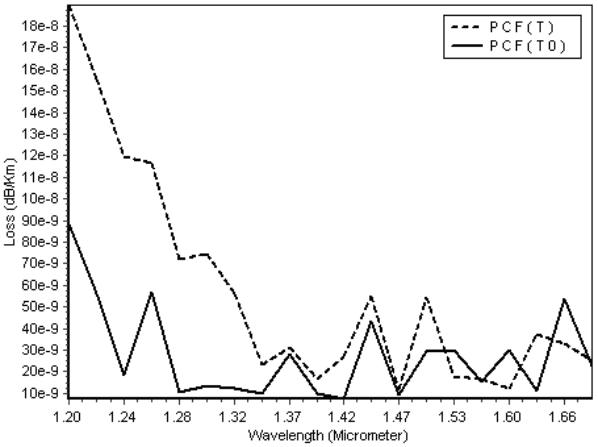

Fig. 9. Confinement loss characteristics as a function of wavelength at room temperature (solid line) and at 500ºK (dash line) for PCF with the following parameters; Λ=3 μm, d_1=1.7 μm and d_2=2.4 μm

hardly changed. Therefore, the effects of temperature increasing and consequently the refractive index contrast increasing on the SMF characteristics is much more than that of PCF.

In the following step of analyzing the photonic crystal fiber, we examine how the total loss in a 90° bend varies as a function of the radius of curvature. The total optical loss as a function of the bend radius of curvature for PCF with Λ=3 μm, d_1=1.7 μm and d_2=2.4 μm at 1.55 μm wavelength is depicted in Fig. 10. As it can be seen, the total loss is decreased by increasing the bend radius of curvature.

Now, we change the geometrical parameters such as the pitch (Λ=1 μm) and the number of air-hole rings (N=6). Fig. 11(a) shows the cross section of the second proposed fiber in which the air-holes diameter of inner ring, d_1 is varied while the other air-holes diameter, d_2 is fixed to 0.8 μm. In the best case, the transversal field intensity distribution for the fundamental guiding mode of designed PCF with d_1=0.39 μm is depicted in Fig. 11(b) which shows the mode is strongly confined.

As it said before, when the air-holes diameter is increased, the air-hole filling factor and consequently the index contrast between the core and the cladding is increased and it has remarkably influences on the PCF characteristics. Figs. 12 and 13 show the loss and dispersion characteristics at room temperature and 500°K respect to wavelength over a wide wavelength range.

The outstanding feature of this fiber is nearly zero dispersion (1.3ps/nm/km at 1.55 μm) along with the low dispersion slope of 0.028 ps/nm^2/km in a wide wavelength rang. Besides, its confinement loss is less than 0.06 dB/km and the effective mode area is 4.462 μm^2.

Also, as shown in Figs. 12 and 13, the effect of temperature variation on the PCF characteristics is too insignificant. So the temperature sensitivity of PCFs is inconsiderable in compare with conventional fibers.

In addition, the total optical loss as a function of the bend radius of curvature for PCF with Λ=1 μm and d_2=0.8 μm, d_1=0.39 μm and N=6 at 1.55 μm wavelength is depicted in Fig. 14. As it can be seen, the total loss is decreased by increasing the bend radius of curvature.

5 Discussion

In this paper, we proposed an efficient SMPCF structure and analyzed its optical properties. Although, there are several reports on design of ultra low and ultra flattened dispersion photonic crystal fibers, but most of the fibers designed in those reports don't provide single mode operation over the C communication band [13, 33-35]. The dispersion of the designed PCF, reported by [13] varies between 0.1 and 0.3 ps/km/nm for the wavelength range from 1.41 to 1.68 μm. Also, the

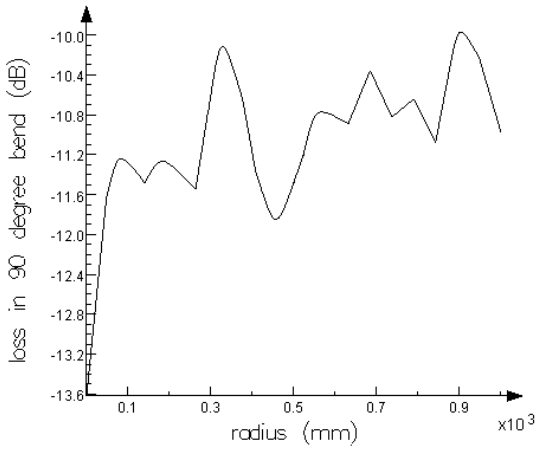

Fig. 10. The total optical loss as a function of the bend radius of curvature for PCF with Λ=3 μm, d_1=1.7 μm and d_2=2.4 μm

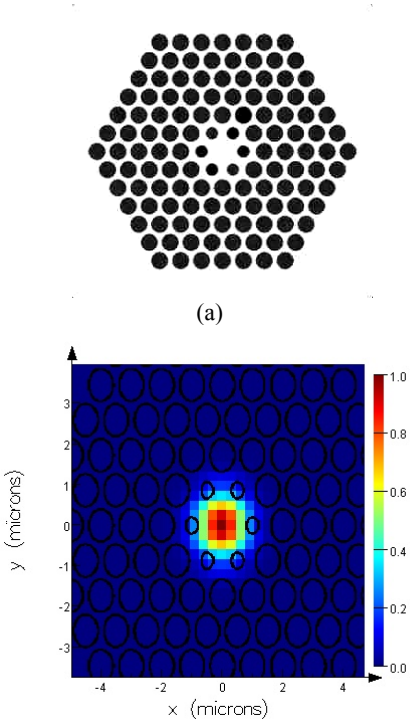

Fig. 11. (a) Section structure of PCF with Λ=1 µm and d_2=0.8 µm, d_1=0.39 µm and N=6 (b) Transversal field intensity distribution for the fundamental guiding mode at 1.55 µm wavelength

confinement loss of the fundamental mode is less than 0.1 dB/km in the wavelength range shorter than 1.7 μm.

In another work in which the air-holes of core region is shrunk to r_c=0.1 µm, the chromatic dispersion changes to positive ranges from 2 ps/km/nm~4.4 ps/km/nm [33]. In [33] dispersion is obtained about 9.8 ps/nm/km with the fluctuation of 0.4ps/nm/km in the C communication band. The designed PCF by Kerrinckx et al [35] has a 9 ring structure with the pitch Λ=2.35 µm and the radius r=0.33 µm. The dispersion of this PCF is 2.5 ps/nm/km at 1.55 µm wavelength.

In several other works, single mode PCFs are studied [36-40], but most of them have investigated either the loss characteristics [36-38] or dispersion characteristics [39-40] and both of these characteristics are not optimized simultaneously. The confinement loss achieved in [36-38] is less than 0.1 dB/km. For the PCF reported in [39], the dispersion and the loss are obtained 16.2 ps/km/nm and 0.19 dB/km respectively. Also a PCF with flattened dispersion of 0.25 ps/km/nm from 1.295 µm to 1.725 µm wavelength is presented in [40].

In this case, a PCF with the loss of 0.06 dB/km, the dispersion of 1.3 ps/nm/km at 1.55 µm wavelength and dispersion slope of 0.028 ps/nm^2/km over a wide wavelength range has been designed. Also the temperature sensitivity of this PCF is much less than that of the conventional fibers.

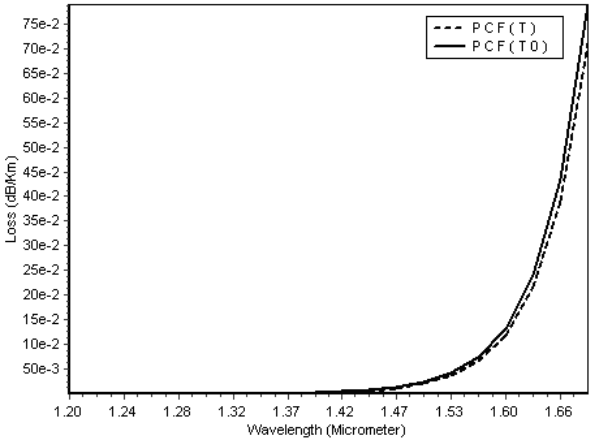

Fig. 12. Confinement loss characteristics as a function of wavelength at room temperature (solid line) and at 500ºK (dash line) for PCF with the following parameters; Λ =1 µm and d_2 = 0.8 µm, d_1 = 0.39 µm and N=6

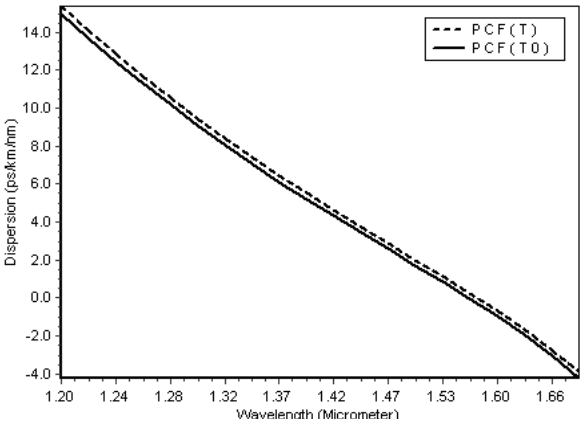

Fig. 13. Dispersion characteristics as a function of wavelength at room temperature (solid line) and at 500ºK (dash line) for PCF with the following parameters; Λ =1 µm and d_2 = 0.8 µm, d_1 = 0.39 µm and N=6

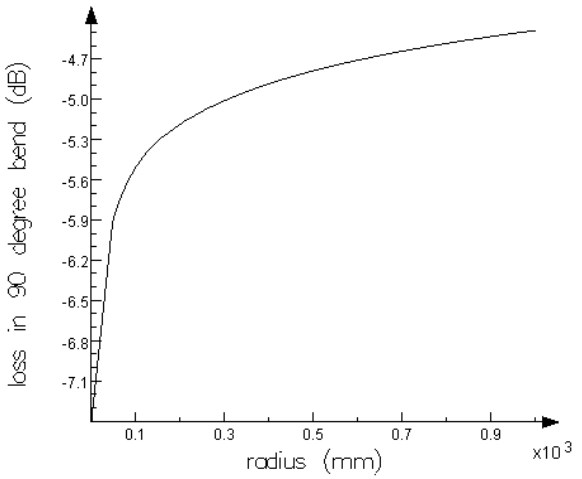

Fig. 14. The total optical loss as a function of the bend radius of curvature for PCF with Λ =1µm and d_2=0.8µm, d_1=0.39 µm and N=6

6 Conclusion

In this article, a novel structure of photonic crystal fiber (PCF) with low confinement loss and nearly zero-flattened dispersion at a wide wavelength range is proposed. The computations based on the FDFD method revealed that the significant characteristics has been obtained by varying the air-holes diameter of the inner rings in the transverse section and increasing the number of air-holes rings. So, a novel PCF with a very low temperature sensitivity and the following characteristics is designed; L=0.06dB/km and D=1.3ps/nm/km at the wavelength of 1.55μm, S=0.028ps/nm^2/km over a wide wavelength range including O, E, S, C, L and U telecommunication wavelength bands. Take all things to account; it is believed that the proposed PCF will have promising future in ultra-broadband transmission applications.

References

[1] Russell P. S. J., "Photonic crystal fibers," *Journal of light wave technology*, Vol. 24, No. 12, pp. 4729-4749, 2006.

[2] Koshiba M. and Saitoh K., "Applicability of classical optical fiber theories to holey fibers," *Opt. Lett.,* Vol. 29, No. 15, pp. 1739–1741, 2004.

[3] Arriaga J., Knight J.C. and Russell P.St.J, "Modellng photonic crystal fibers," *Physica E 17, Elsevier Science*, pp. 440-442,2003.

[4] Soussi S., "Modellng photonic crystal fibers," *Applied mathematics, Elsevier Science*, pp. 288-317, 2005.

[5] Calo G., Dorazio A., De Sario M., Mescia L., Petruzzelli V. and Prudenzano F., "Photonic crystal fibers," *ICTON*, pp. 115-120, 2005.

[6] Pourmahyabadi M. and Mohammad Nejad S., "Design of Single Mode Photonic Crystal Fibers with Low-Loss and Flattened Dispersion at 1.55μm Wavelength," *Proceeding on the 4th International Symposium on High Capacity Optical Networks and Enabling Technologies*, November 18-20, Dubai, UAE, 2007.

[7] Pourmahyabadi M. and Mohammad Nejad S., "Numerical Investigation and Optimization of a Photonic Crystal Fiber with Ultra-Low Confinement Loss and Ultra-Flattened Dispersion". *Proceeding on The 6th International Symposium on Communication Systems, Networks and Digital Signal Processing,* pp. 557-561, CSNDSP, Graz, Austria, July 2008.

[8] Pourmahyabadi M. and Mohammad Nejad S., "Optimal confinement loss reduction in photonic crystal fiber with ultra-flattened dispersion," *Proceeding on the Symposium on High Capacity Optical Networks & Enabling Technologies,* pp. 265-270,18-20 November, HONET 08, Penang, Malaysia, 2008.

[9] Aliramezani M., Mohammad Nejad S. and M. Pourmahyabadi, "Design of photonic crystal fiber with improved dispersion and confinement loss over all telecommunication bands," *Proceeding on the Symposium on High Capacity Optical Networks & Enabling Technologies*, pp. 141-145, 18-20 November, HONET 08, Penang, Malaysia, 2008.

[10] Zhu Z. and Brown T. G., "Analysis of the fundamental space-filling mode of photonic crystal fibres: a symmetry point of view," *Opt. Express*, No. 10, pp. 853–64, 2002.

[11] Zhu Z. and Brown T. G., "Full-vectorial finite-difference analysis of microstructured optical fibers," *Opt. Express*, Vol. 10, No. 17, pp. 853-864, 2002.

[12] Guo S., Wu F. and Albin S., "Photonic band gap analysis using finite difference frequency-domain method," *Opt. Express*, Vol. 12, No. 8, pp. 1741-1746, 2004.

[13] Saitoh K. and Koshiba M., "Numerical modeling of photonic crystal fibers," *Lightwave Technology*, Vol. 23, No. 11, pp. 3580-3590, 2005.

[14] Poletti F., FinazziV., Monro T. M., Broderick N.G.R., TseV. and Richardson D. J.; "Inverse design and fabrication tolerances of ultra-flattened dispersion holey fibers," *Opt. Express*,Vol. 13, No. 10, pp. 3728-3736, 2005.

[15] Simmons J. H. and Potter K. S., "*Optical Materials*," Academic Press, An Imprint of Elsevier, San Diego, 2000.

[16] Weber M. J., *"Handbook of Optical Materials,"* Chapter 2, The CRC Press, 2002.

[17] Wakaki M., Kudo K., Shibuya T., *"Physical properties and data of optical materials,"* The CRC Press, 2007.

[18] Saitoh K. and Koshiba M., "Chromatic dispersion control in photonic crystal fibers: application to ultra-flattened dispersion," *Optics Express*, Vol. 11, pp. 843–852, 2003.

[19] Renversez G., Kuhlmey B. and McPhaedran R., "Dispersion Management with microstructured optical fibers: ultraflattened chromatic dispersion with low losses," *Opt. Lett*. 28, pp. 989-991, 2003.

[20] Zolla F., Renversez G., Nicolet A., kuhlmey B., Guenneau S. and Felbacq D., *"Foundation of Photonic Crystal Fibers, "* Chapter 7, pp. 247-249, Imperial College Press, 2005.

[21] Goncharenko I. A., Helfert S. F . and Pregla R., "Radiation Loss in Curved Holey Fibres," *ICTON*, IEEE, pp. 220-223, 2003.

[22] Nielsen M. D., Mortensen N. A., Albertsen M., Folkenberg J. R., Bjarklev A., Bonacinni D., "Predicting macrobending loss for large-mode

area photonic crystal fibers," *Opt. Express*, Vol. 12, No. 8, pp. 1775-1779, 2004.

[23] Baggett J. C., Monro T. M., Furusawa K., Finazzi V. and Richardson D.J., "Understanding bending losses in holey optical fibers," *Optics Communications,* Vol. 227, pp. 317–335, 2003.

[24] Sørensen T., Broeng J., Bjarklev A., Knudsen E. and Libori S. E. B., "Macro-bending loss properties of photonic crystal fibre," *Electron. Lett*. Vol. 37, pp. 287–289, 2001.

[25] Sørensen T., Broeng J., Bjarklev A., Hansen T. P., Knudsen E., Libori S. E. B., Simonsen H. R. and Jensen J. R., "Spectral Macro-bending loss considerations for photonic crystal fibres," *IEE Proc.-Opt.* Vol. 149, pp. 206-210, 2002.

[26] Belhadj W., AbdelMalek F., Bouchriha H., "Characterization and study of photonic crystal fibres with bends," *Materials Science and Engineering C,* Vol. 26, pp. 578–579, 2006.

[27] Tan X., Geng Y., Li E., Wang W., Wang P. and Yao J., "Characterization of bent large-mode-area photonic crystal fiber," *J. Opt. A: Pure Appl. Opt.* Vol. 10, 2008.

[28] http://www.lumerical.com/mode_online_help/usr_waveguide_bend.php.

[29] Zhu Y., Chen Y.; Huray P. and Dong X.; "Application of a 2D-CFDTD Algorithm to the Analysis of Photonic Crystal Fibers (PCFs)," *Proceedings IEEE, Southeastcon,* pp. 215-219, 2002.

[30] Florous N. J.,Varsheney S. K., Saitoh K. and Koshiba M., "Thermooptical Sensitivity Analysis of Highly Birefringent Polarimetric Sensing Photonic Crystal Fibers With Elliptically Elongated Vein," *IEEE Photonics Technology Letters*, Vol. 18, No. 15, pp. 1663-1665, 2006.

[31] Shima K., Himeno K., Sakai T., Okude S., Wada A. and Yamauch R., "A novel temperature-insensitive long-period fiber grating using a boron-codoped-germano silicate-core," *OFC Technical Digest*; pp. 347-348, 1997.

[32] Bhatia V., Campbell D. K., D'Alberto T., Eyck G. A. T., Sherr D., Murphy K. A. and Claus R. O., "Standard optical fiber long-period gratings with reduced temperature sensitivity for strain and refractive-index sensing," *OFC Technical Digest;* pp. 346-347, 1997.

[33] Guoa S., Anb W., Wang K., Zhu G. and Le Z., "Large Area Model Field Photonic Crystal Fiber Design," *Proc. of SPIE*, Vol. 6019, pages 60193Y, 2005.

[34] Shuqin G., Zichun L. and Bisheng Q., "Realization of Ultra-broadband Dispersion-flattened in Dual-cladding Photonic Crystal Fiber," *Proc. of SPIE*, Vol. 6025, pages 602504, 2006.

[35] Kerrinckx E., Bigot L., Douay M. and Quiquempois Y., "Photonic crystal fiber design by means of a genetic algorithm," *Optics Express*, 2004, Vol. 12, No. 9, pp. 1990-1995, 2004.

[36] Zhang F., Liu X., Zhang Z., Zhang M., Ye P., "A novel single-polarization single-mode photonic crystal fiber," *Proc. of SPIE*, Vol. 6351, pages 63512Q, 2006.

[37] Saitoh K. and Koshiba M., "Single-Polarization Single-Mode Photonic Crystal Fibers," *IEEE Photonics Technology Letters,* Vol. 15, No. 10, pp. 1384-1386, 2003.

[38] Ju J., Jin W. and Demokan M. S., "Design of Single-Polarization Single-Mode Photonic Crystal Fiber at 1.30 and 1.55μm," *Journal of Lightwave Technology,* Vol. 24, No. 2, pp. 825, 2006.

[39] Nakajima K., Zhou J., Tajima K., Kurokawa K., Fukai C. and Sankawa I., "Ultrawide-Band Single-Mode Transmission Performance in a Low-Loss Photonic Crystal Fiber," *Journal of Lightwave Technology,* Vol. 23, No. 1, 7-, 2005.

[40] Wu T. L. and Chao C. H., "A Novel Ultraflattened Dispersion Photonic Crystal Fiber," *IEEE Photonics Technology Letters,* Vol. 17, No. 1, pp. 67-69, 2005.

Maryam Pourmahyabadi received the B.Sc. degree from Shahid Bahonar University, Kerman, Iran, the M.S. degree from Guilan University, Rasht, Iran, both in Electronics Engineering, in 1997 and 2000 respectively. She is currently working toward the Ph.D degree in Electronics Engineering with Iran university of Science and Technology, Tehran, Iran. Her present research interests include optical components/subsystems for optical fiber communication and fiber sensors.

Shahram Mohammad Nejad received his B.Sc. in Electrical Engineering from University of Houston, Houston, USA, in 1981 and M.S. and Ph.D. degrees in Semiconductor Material Growth and Lasers from Shizuoka University, Shizuoka, Japan, in 1990 and 1993, respectively. Professor Mohammad Nejad invented the PdSrS laser for the first time in 1992. He has published over 80 scientific papers and books. Currently, he is the Head of Electrical Engineering Department, Iran University of Science and Technology, Tehran, Iran. Also, he is a scientific committee member of Iranian Conference on Electrical Engineering (ICEE) and also Iranian Conference on Optics & Photonics, member of Institute of Engineering and Technology (IET) and an IET-CEng. His research interests include semiconductor material growth, quantum electronics, semiconductor devices, optoelectronics, electronic devices and lasers.